



Genesis of Tropical Storm Eugene (2005) from Merging Vortices Associated with ITCZ Breakdowns. Part III: Sensitivity to Various Genesis Parameters

CHANH Q. KIEU* AND DA-LIN ZHANG

Department of Atmospheric and Oceanic Science, University of Maryland, College Park, College Park, Maryland

(Manuscript received 12 June 2009, in final form 23 January 2010)

ABSTRACT

In this study, a series of sensitivity simulations is performed to examine the processes leading to the genesis of Tropical Storm Eugene (2005) from merging vortices associated with the breakdowns of the intertropical convergence zone (ITCZ) over the eastern Pacific. This is achieved by removing or modifying one of the two vortices in the model initial conditions or one physical process during the model integration using the results presented in Parts I and II as a control run. Results reveal that while the ITCZ breakdowns and subsequent poleward rollup (through a continuous potential vorticity supply) provide favorable conditions for the genesis of Eugene, the vortex merger is the most effective process in transforming weak tropical disturbances into a tropical storm. The sensitivity experiments confirm the authors' previous conclusions that Eugene would not reach its observed tropical storm intensity in the absence of the merger and would become much shorter lived without the potential vorticity supply from the ITCZ.

It is found that the merging process is sensitive not only to larger-scale steering flows but also to the intensity of their associated cyclonic circulations and frictional convergence. When one of the vortices is initialized at a weaker intensity, the two vortices bifurcate in track and fail to merge. The frictional convergence in the boundary layer appears to play an important role in accelerating the mutual attraction of the two vortices leading to their final merger. It is also found from simulations with different storm realizations that the storm-scale cyclonic vorticity grows at the fastest rate in the lowest layers, regardless of the merger, because of the important contribution of the convergence associated with the boundary layer friction and latent heating.

1. Introduction

It is well known that tropical cyclogenesis (TCG), a process by which weak tropical disturbances are transformed to a self-sustaining tropical cyclone (TC), is much less deterministic than the track and intensity of mature hurricanes, even with the incorporation of all available remote sensing and in situ observations. In particular, there are many tropical disturbances propagating in climatologically favorable environments each year—for instance, in the vicinity of the intertropical convergence zone (ITCZ)—but only a small fraction of them can fully develop into TCs (Gray 1968; McBride and Zehr 1981;

Molinari et al. 2000; DeMaria et al. 2001). So far, our understanding of the processes leading to the developing versus nondeveloping systems still remains elusive because of the lack of detailed observations at their birthplaces.

Lander and Holland (1993) are perhaps among the first to notice from the early Tropical Cyclone Motion-90 field experiment (TCM-90; Elsberry 1990) that there is often a pool of mesovortices in a monsoon trough preceding the formation of a TC. The interactions and mergers of these vortices have since received more attention in recent observational studies, as there is growing evidence that these vortices could play an important role in TCG (e.g., Simpson et al. 1997; Ritchie and Holland 1997, hereafter RH97; Reasor et al. 2005). Such mesoscale merging processes are fundamentally different from hurricane-like vortex–vortex interactions (e.g., Fujiwhara 1921, 1923; Ritchie and Holland 1993; Wang and Holland 1995) because these mesoscale disturbances have smaller scales and less organized structures than typical TC-like vortices and often exhibit rapid transformations during their early developments.

* Current affiliation: Department of Meteorology, College of Science, Vietnam National University, Hanoi, Vietnam.

Corresponding author address: Dr. Da-Lin Zhang, Department of Atmospheric and Oceanic Science, University of Maryland, College Park, College Park, MD 20742–2425.
E-mail: dalin@atmos.umd.edu

In the study of the genesis of Typhoon Irving, RH97 showed that the interaction of a low-level circulation with an upper-level trough could lead to the development of a tropical depression, and the subsequent merger of two midlevel mesovortices within this depression gave rise to the intensification of Irving to tropical storm (TS) intensity. RH97 hypothesized that the vorticity growth associated with the merger occurred from the top downward as a result of the increased penetration depth. Although such a vortex–vortex interaction played an important role in Irving’s intensification to TS intensity, how the merging vortices interacted with the low-level background flows in the context of vorticity dynamics was not shown because of the lack of high-resolution observations.

A recent study of Wang and Magnusdottir (2006) provides some other clues to TCG occurring over the eastern Pacific where most of the TCG events are statistically related to easterly disturbances causing the ITCZ breakdowns rather than to the internal dynamic instability of the ITCZ as described by Nieto Ferreira and Schubert (1997). Unlike the case of Typhoon Irving in which the merging mesovortices within a monsoon trough are confined at the midlevel (RH97), tropical disturbances over the eastern Pacific are often characterized by mesoscale cyclonic circulations in the lower troposphere due to the shallow nature of the trade winds (e.g., Serra and Houze 2002). Their interactions and some other processes leading to TCG in this region are the subject of the present study.

In Parts I and II of this series of papers (i.e., Kieu and Zhang 2008, 2009, hereafter Part I and Part II, respectively), we investigated the genesis of TS Eugene (2005) that occurred during the National Aeronautics and Space Administration’s (NASA’s) Tropical Cloud Systems and Processes (TCSP; Halverson et al. 2007) field campaign over the eastern Pacific using satellite observations, the National Centers for Environmental Predictions (NCEP) reanalysis, and a 4-day (0000 UTC 17 July–0000 UTC 21 July 2005) cloud-resolving simulation with the Advanced Research Weather Research and Forecasting model (ARW-WRF). The simulation with multinested (36/12/4/1.33) km grids captures well main characteristics of the storm during its life cycle from the early genesis to the dissipation stages without bogusing any data into the model initial conditions. Both the observations and model simulation show the merger of two mesovortices (hereafter V_1 and V_2) associated with the ITCZ breakdowns during the formation of TS Eugene (see Fig. 1a). Here the merging period begins as V_2 ’s southerly flow decreases in intensity and coverage with the approaching of V_1 and ends when only one circulation center appears at 850 hPa (see Figs. 10 and 11 in Part I). The two mesovortices are merged at 39 h into the integration, valid at

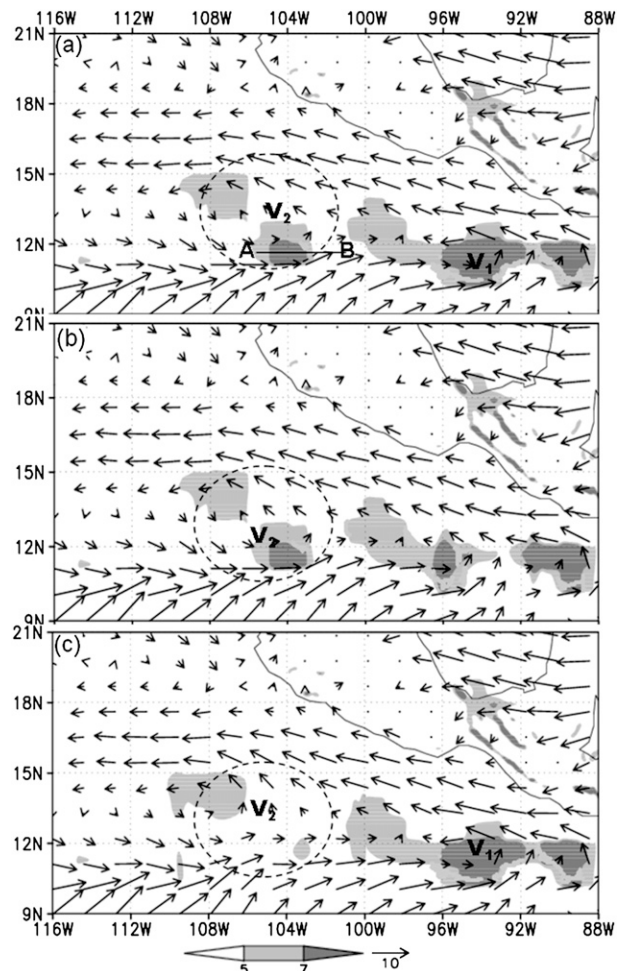


FIG. 1. The model initial conditions (i.e., at 17/00–00) of the vertical relative vorticity (shaded, 10^{-5} s^{-1}) and flow vectors (m s^{-1}) in the surface layer for (a) the control (CTL) run, (b) the MV2 run in which V_1 is removed, and (c) the WV2 run in which V_2 is weakened after removing a smaller-scale vortex in the south-eastern quadrant of the dashed circle. The dashed circles denote roughly the area where a midlevel mesovortex associated with V_2 would develop at the later time. Line AB in (a) denotes the location of the cross section shown in Fig. 2.

1500 UTC 18 July 2005 (hereafter 18/15–39), mostly because of their different larger-scale steering flows. That is, V_1 moves northwestward and coalesces with and is then captured by V_2 moving slowly north-northeastward. We have demonstrated in Part II that unlike the conceptual models of vortex mergers in the barotropic framework (e.g., Holland and Dietachmayer 1993; Prieto et al. 2003; Kuo et al. 2008), the merging process in the present case is characterized by sharp increases in the surface heat fluxes, the low-level convergence, latent heat release (and upward motion), the low to midtropospheric potential vorticity (PV), surface pressure fall, and the rapid growth of cyclonic vorticity in the lower troposphere.

TABLE 1. Description of sensitivity experiments, including the minimum central pressure P_{\min} (hPa) and the maximum surface wind V_{\max} (m s^{-1}) during the life cycle of each storm.

Expt	Description	P_{\min}	V_{\max}
CTL	Control run	986	38
MV2	V_1 is partially removed from the initial conditions	995	21
WV2	Only one subvortex embedded within V_2 is removed	996	20
WSST	The SST field to the north of the storm is set at 301 K.	969	52
WST-V2	As in MV2, except for the SST field that is set the same as that in WSST	986	35
RFRC	Frictional terms in the horizontal momentum equations are reduced exponentially with time after 17/18–18	997	39
RPVF	The PV flux from the ITCZ is reduced exponentially, starting from 14°N southward and after 19/12–36	995	23

Our PV budget calculations in Part II show two different episodes of the storm intensification. That is, the vortex merger results in a surge of PV flux into the storm circulation that produces about a 10-hPa central pressure drop (i.e., from 18/12–36 to 19/00–48), whereas the subsequent PV supply from the ITCZ contributes significantly to the continued intensification of the storm—that is, with another 7–8 hPa drop (between 19/03–51 and 19/15–63) even after it moves over a cooler sea surface. The vorticity budget shows that the cyclonic vorticity growth from the merger occurs from the bottom upward, which is consistent with the previous studies of TCG from a midlevel convectively generated mesovortex (MCV) by Zhang and Bao (1996a,b) and from a large-scale frontal system by Hendricks et al. (2004).

It is also shown in Part II that the vortex merger occurs as the gradual capture of small-scale (i.e., 10–40 km) PV patches within V_2 by the fast-moving V_1 , giving rise to high PV near the merger's circulation center, with its peak amplitude located slightly above the melting level. This vertical PV structure leads us to view the two vortices as midlevel MCVs. However, an examination of NCEP's reanalysis and the model simulation up to 18/00–24 (i.e., about 6 h prior to the merger) indicates that only V_2 may be considered as a midlevel mesovortex consisting of several subvortices with much less organized circulations in the lower troposphere (see Figs. 10 and 11 in Part I and Fig. 3a herein). By comparison, V_1 is more or less a lower tropospheric mesovortex in terms of the relative vorticity and circulation, and its low-level characteristic is well preserved before and during its interaction with V_2 (see Fig. 3 in Part I and Fig. 3b herein). Although V_1 forms a well-defined surface circulation with maximum surface winds reaching 13–14 m s^{-1} prior to the merger, V_2 shows little evidence of closed surface isobars until about 12 h into the integration. In addition, the latter's closed surface isobars begin to diminish because of the reduced convective activity when V_1 is in close proximity (see Fig. 10 in Part I). Thus, TS Eugene should be regarded as the merger of a midlevel

and a low-level mesovortex or simply as the merger of two mesovortices.

In Part III of this series of papers, we wish to address the following questions, based on the results presented in Parts I and II: How critical is the vortex merger in the formation of TS Eugene? That is, could Eugene be developed from one of the mesovortices without merging with the other one? To what extent do the convectively generated PV fluxes in the ITCZ assist the deepening of Eugene, especially after its migration into an environment with strong vertical shear and colder sea surface temperature (SST)? What are the roles of the frictional convergence in the planetary boundary layer (PBL) in determining the genesis of Eugene? Is the bottom-up development of Eugene valid in general or is it just a result of the vortex merger? These questions will be addressed through a series of sensitivity simulations by turning off a genesis parameter (or one physical process) in the initial conditions (or during the model integration) of each simulation while keeping all the other parameters (processes) identical to the control simulation (CTL) presented in Parts I and II.

The next section describes experimental designs. Section 3 discusses in depth the outcomes of each sensitivity experiment and its implications. Section 4 examines the growth of the storm-scale cyclonic vorticity from some sensitivity simulations, as compared to that from the control simulation. A summary and concluding remarks are given in the final section.

2. Experimental designs

A total of six sensitivity simulations, summarized in Table 1, are conducted to examine the sensitivity of the model-simulated Eugene to various genesis parameters. They include the effects of removing each mesovortex (i.e., V_1 or V_2), the PV supply from the ITCZ, the frictional convergence in the PBL, and changing SST. We hope that results from these experiments could also help reveal the predictive and stochastic aspects of

TCG. The associated experiment designs are described below.

a. Removal of each of the mesovortices

Since TS Eugene deepens most significantly during the merging stage, it is natural to examine how critical the merger is. To this end, we first need to remove one of the mesovortices in each sensitivity simulation to see if the other mesovortex could alone grow to the intensity of Eugene as in CTL. In addition, its comparison with the CTL run will allow us to investigate the relative importance of the merger versus the ITCZ rollup in the genesis of Eugene. Here we follow the procedures of Kurihara et al. (1993) to remove a vortex from the model initial conditions by performing the following steps: (i) remove the large-scale mean flows within a selected domain that encloses the vortex of interest; (ii) extract and then remove the axisymmetric component of the vortex from the perturbation flows after performing the azimuthal Fourier decomposition; and (iii) add the large-scale mean flows back to the initial conditions to ensure that the ambient flow conditions are preserved. The mass field is modified in accordance with the gradient wind balance with the removed wind field. However, the initial relative humidity is kept unchanged to minimize the initial cloud-precipitation spinup differences between the CTL and sensitivity simulations. To remove a mesovortex as smoothly as possible, we use a cutoff function of the form $e^{-(r/R)^2}$, where R is the outer radius of each mesovortex to be removed (100 km for V_1 and 250 km for V_2). Figures 1a and 1b compare the vertical relative vorticity at the initial time between CTL and a sensitivity simulation in which V_1 is removed (MV2). Clearly, the vortical flows of V_1 are substantially reduced. However, some shear vorticity is still present, which represents roughly the larger-scale horizontal sheared flows associated with the ITCZ.

Because of the two different sizes and kinematical characteristics of V_1 and V_2 , it is also desirable to see if V_1 could develop into TS intensity in the absence of V_2 . However, removing the vortical flows of V_2 is not as straightforward as those of V_1 because V_2 is not well defined at the initial time. Although the initial vorticity field given in Fig. 1a appears to indicate two smaller-scale vortices within an area (circled) where V_2 develops, a closed circulation of V_2 is not seen from the simulation until 12 h into integration. Our experimentation with the removal of V_2 's background cyclonic flows ranging from 250 to 500 km in radius shows that the elongated shear vorticity associated with the ITCZ could hardly be eliminated completely, just as with V_1 (cf. Figs. 1a and 1b). As a result, the initial cyclonic vorticity within V_2 , as seen in Fig. 1a, could spin up numerous small-scale vortices, and

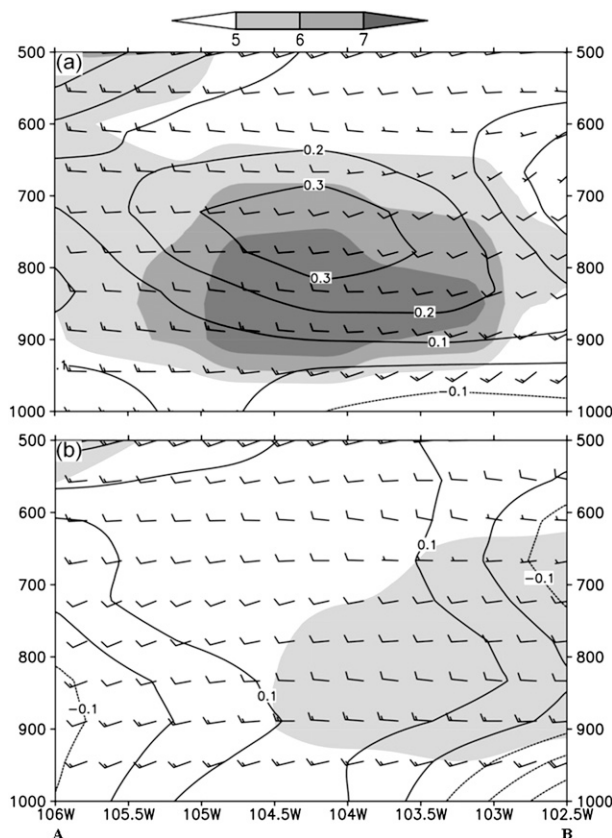


FIG. 2. Vertical cross section of the vertical relative vorticity (shaded, 10^{-5} s^{-1}) and the potential temperature anomaly (contoured at intervals of 0.1°C) along line AB, as given in Fig. 1a, associated with a subvortex in the model initial conditions (i.e., at 17/00–00) for the (a) CTL and (b) WV2 runs. Horizontal wind bars are superimposed; a full barb is 5 m s^{-1} .

their subsequent merger could still lead to the development of a new mesovortex that is similar to V_2 in CTL, albeit with weaker intensity (not shown).

With such an ambiguity in defining V_2 at the initial condition, we found, however, that removing one major subvortex within the area where V_2 is about to develop is sufficient to reduce the strength of V_2 substantially at later times, which in turn affects the evolution of V_1 prior to the merging phase. Therefore, another sensitivity simulation (WV2) is performed in which V_2 is made weaker than that in CTL by removing a subvortex while leaving all the other features intact. Figure 2 compares the vertical vorticity structures before and after the removal. The removed vortex is initially located at the central portion of the ITCZ (and V_2) with a radius of about 100 km (Fig. 1a), and it is partially removed after applying the above procedures (cf. Figs. 1a and 1c). A balanced warm core associated with the subvortex ($>0.3^\circ\text{C}$), centered at 750 hPa, is also eliminated in accordance with the removed rotational flows of V_2 (cf. Figs. 2a and 2b). Again,

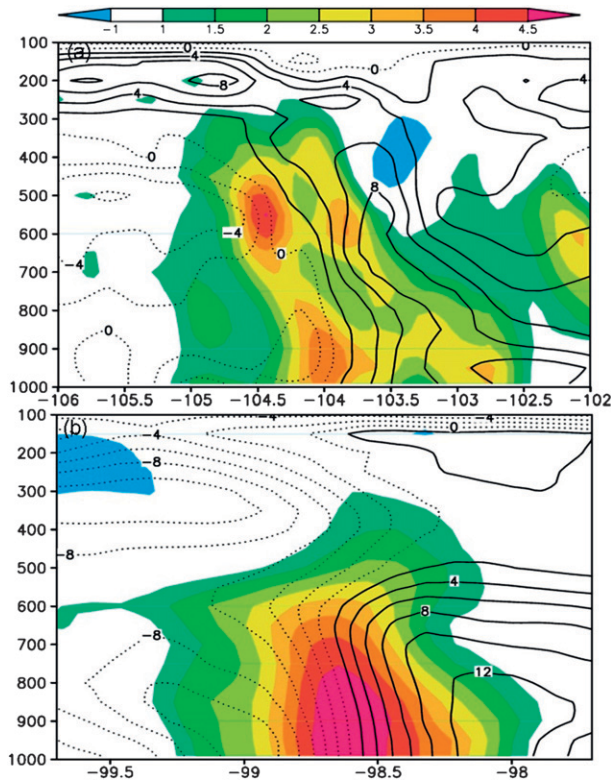


FIG. 3. West-east vertical cross section of the vertical relative vorticity (shaded at intervals of $5 \times 10^{-5} \text{ s}^{-1}$) and the tangential wind relative to the mean flows (contoured at interval of 2 m s^{-1}) through the centers of (a) V_2 and (b) V_1 , valid at 18/00–24 when both vortices are about 750 km apart.

there is little change in the larger-scale flow field before and after the removal.

b. Use of a warmer SST

As shown in Part I, Eugene dissipates quickly after moving northwestward into an environment with strong vertical shear and a cooler sea surface (i.e., cooler than 26.5°C). To examine the relative roles of the vertical wind shear and SST, a sensitivity experiment (WSST) is carried out in which SST over the 4-km resolution domain is set at a tropical value of no less than 301 K to see if Eugene could continue to intensify even in the presence of the same strong vertical shear as that in CTL. Through this experiment, we wish to isolate the roles of SST versus vertical wind shear in determining the development of Eugene.

Because both the vortex merger and ITCZ rollup are allowed in WSST, another experiment (WST_V2) is conducted in which V_1 is removed as in MV2 but SST is modified as in WSST, in an attempt to isolate the relative roles of vortex merger, warm SST, and the ITCZ rollup during the genesis stages of Eugene. Strictly speaking, the

results so obtained could not be directly compared to those in CTL because of the two genesis parameters being simultaneously removed in one simulation, unless a factor separation scheme of Stein and Alpert (1993) is applied. However, by comparing the WST_V2 storm to the MV2 storm, we could see if V_2 from the ITCZ breakdown could grow at a much faster rate than the MV2 storm, given all the possibly favorable conditions, and if so, how long it would take for such a breakdown to reach TS intensity under the present eastern Pacific conditions. On the other hand, a comparison between WST_V2 and WSST will allow us to assess the efficiency of the ITCZ rollup versus vortex merger in the development of Eugene from a weak disturbance to a tropical storm over the same tropical ocean surface.

c. Diminished frictional convergence in the PBL

Craig and Gray (1996) provided a lucid study about the distinction between two principal theories of TC development: the wind-induced surface heat exchange (WISHE) proposed by Emanuel (1987) and conditional instability of the second kind (CISK) suggested by Charney and Eliassen (1964). The main conceptual difference between the two theories lies in the feedback loop connecting TC development to the PBL processes (i.e., moist convergence associated with the radial frictional convergence versus surface heat exchange associated with the tangential flows). Because the two processes depend on the momentum drag and the heat and moisture exchange coefficients, respectively, Craig and Gray (1996) conducted a series of sensitivity experiments in which these coefficients are varied alternately. Their results confirm the WISHE feedback as the main mechanism for TCG. In fact, we have also seen in Part II that the surface heat fluxes and pressure drops increase sharply during the merging phase, also revealing the important roles of the WISHE process in the genesis of Eugene.

While the WISHE theory has been widely regarded as the main feedback mechanism for TCG, Craig and Gray (1996) cautiously emphasized that the ineffectiveness of the CISK process that they estimated is only valid if the constant moisture content [or convective available potential energy (CAPE)] can be maintained during the model integrations. So it is still unclear if WISHE could be the dominant process leading to TC development without the CISK contribution. Given their idealized model configurations, it would be of interest to see if Craig and Gray's conclusions about the effects of frictional convergence are also valid in the present real-data case study. Thus, a sensitivity simulation (RFRC) is conducted in which the entire PBL frictional effects in the horizontal momentum equations are reduced gradually to zero after the merger, but calculations of the surface sensible and

latent heat fluxes in the thermodynamic and moisture conservation equations are kept the same as in CTL. This experiment will help elucidate the relative importance of the frictional convergence versus the surface heat exchange in the genesis of Eugene. To minimize any imbalance from an abrupt removal of the frictional forcing prior to the vortex merger, the PBL frictional effects are gradually reduced, starting from 18 h into the integration, by multiplying a factor $\mu = e^{-\alpha t}$ to the total PBL frictional forcing, where α is the inverse of an e -folding time scale and is set to $(18 \text{ h})^{-1}$. This implies that the PBL frictional effects will be reduced by e^{-1} at 18/12–36 and become negligible after 19/06–54. Apparently, this sensitivity experiment differs from those experiments conducted by Craig and Gray (1996) in which the drag coefficient is only varied in magnitude rather than diminished to null as in our experiment.

d. Reduced PV supply from the ITCZ

Our PV budget calculations, given in Part II, show that the continuous south-to-southwesterly PV flux from the ITCZ into Eugene's circulation appears to account for the continued deepening of Eugene after its propagation into an unfavorable environment. From the PV viewpoint, such deepening could be understood in the context of balanced dynamics for the increased PV in a given volume. In essence, the larger the amplitude of the mean PV in the volume, the stronger the induced balanced circulation and temperature perturbation will be (Hoskins et al. 1985). It was hypothesized that Eugene would become shorter-lived without the continuous PV fluxes from the ITCZ. To validate this hypothesis, a sensitivity simulation (RPVF) is performed in which the PV generation in the ITCZ is reduced after the merger. Since PV is generated mostly by latent heat release, we impose a latitude-dependent damping to the heat source term in the thermodynamic equation. The damping parameter $\Gamma(y)$ takes the form of

$$\Gamma(y) = \exp\left[-\left(\frac{y - y_0}{L}\right)^4\right],$$

where y is latitude, y_0 is a reference latitude chosen to be the northern boundary (at 30°N) of the 12-km resolution domain (see Fig. 4 in Part I), and L is the scale of the damping that is assumed to be half of the width of the 12-km-resolution domain (i.e., about 1500 km). This damping parameter will gradually reduce the latent heating rates, starting from 14°N southward where the ITCZ resides, while preserving the heating rates to its north. This damping is activated about 18/12–36 to ensure a smooth transition after the merger. Note that this damping does not apply to the water vapor conservation equation, so that water vapor will still be advected into the storm in

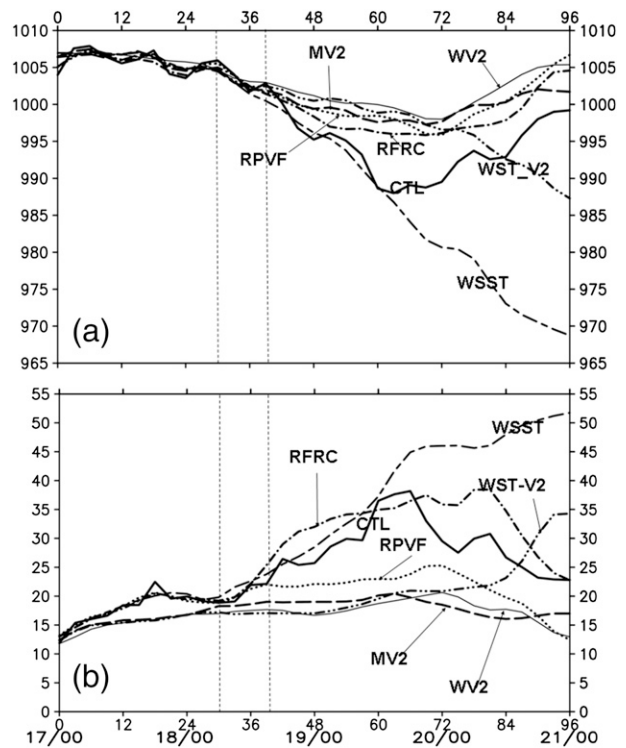


FIG. 4. Time series of (a) the simulated minimum sea level pressure (hPa) during the 4-day period of 17/00–00 to 21/00–96 from the numerical experiments of CTL (thick solid), MV2 (long dashed), WV2 (thin solid), WSST (short-long dashed), WST-V2 (double-dot-dashed), RPVF (dotted), and RFRC (dot-dashed). The merging phase is denoted by the vertical dashed lines. (b) As in (a), but for the maximum surface (absolute) wind.

the same manner as that in CTL. Any condensation corresponding to the reduced latent heat release within the damping region will be removed as precipitation reaching the surface to eliminate its water loading effects on the circulation of Eugene.

3. Results

The sensitivity of the genesis of Eugene to the different TCG parameters described in the preceding section can be evaluated through the time series of the intensity, track, and surface heat fluxes (Figs. 4, 5 and 6). Table 1 lists the maximum intensities during the life cycles of the simulated storms. In addition, Fig. 5 compares the simulated surface circulations at 18/06–30, at which time the two mesovortices in CTL are in close proximity. In general, one can see from the sensitivity experiments that the circulation patterns diverge remarkably, depending mainly on whether or not the merger could occur, whereas their tracks at the later stages depend upon their different intensities (i.e., more westward than northwestward for weaker storms; Fig. 5). More details are discussed below.

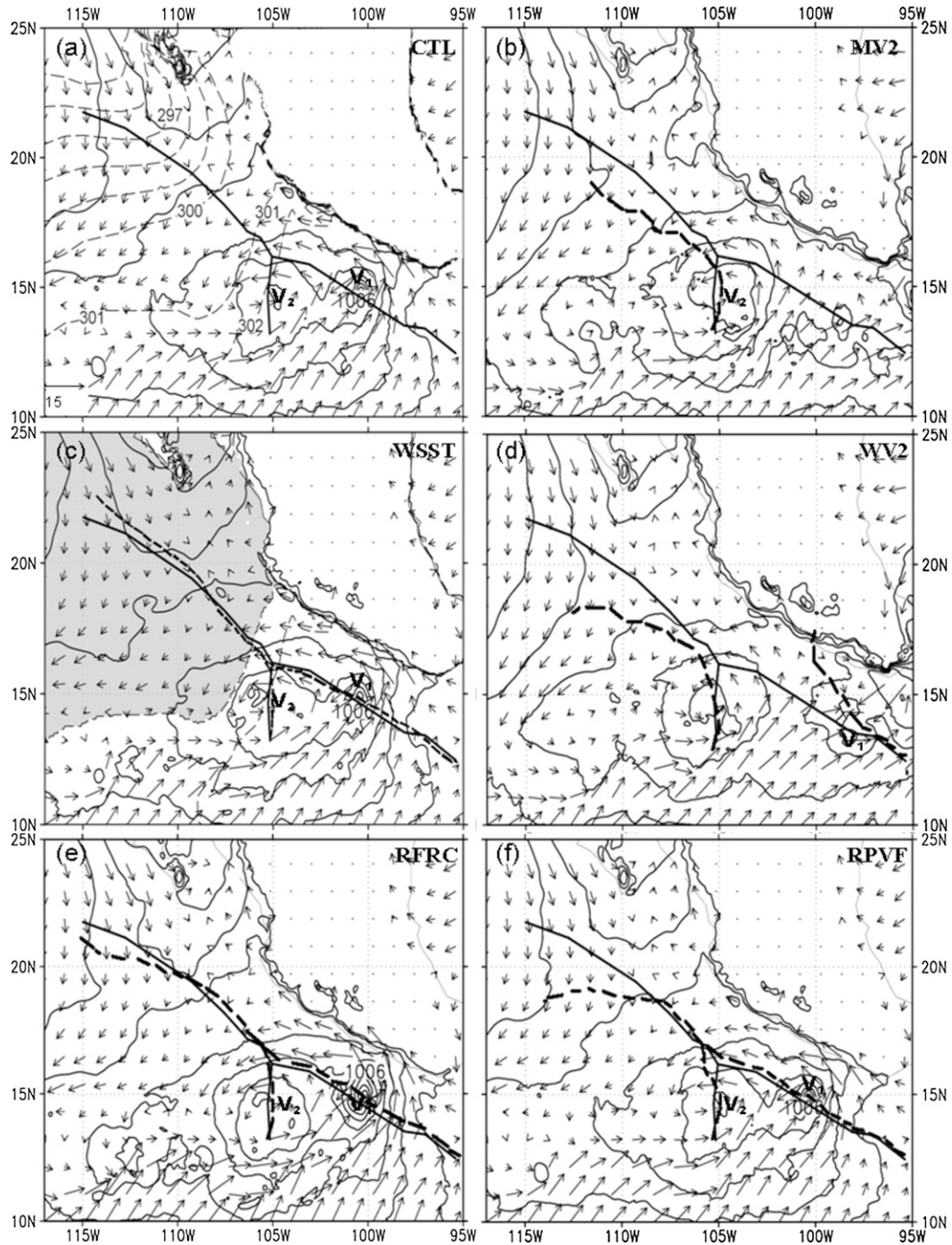


FIG. 5. Comparison of the simulated tracks between CTL (solid) and each sensitivity run (dashed), superimposed with the surface flow vectors [the reference vector is at the bottom left corner of (a), $m s^{-1}$] and sea level pressure (every 1 hPa), valid at 18/06–30, from the (a) CTL (control); (b) MV2 (V_1 removed); (c) WSST (SST = 301 K); (d) WV2 (a weaker V_2); (e) RFRC (diminished PBL friction); and (f) RPVF (reduced PV flux from the ITCZ) simulations. Dashed lines in (a) and (c) denote the distribution of SST; the gray area in (c) denotes the area of SST = 301 K.

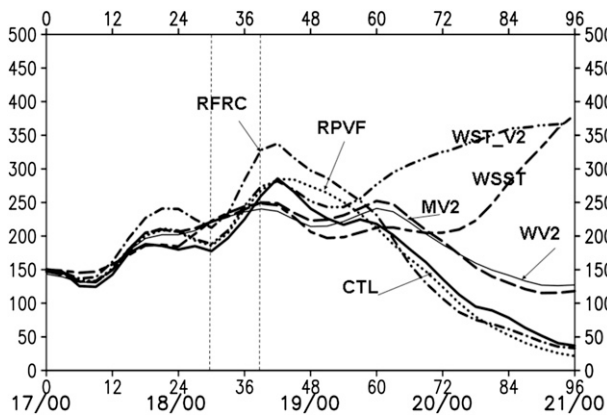


FIG. 6. Time series of the ($720 \text{ km} \times 720 \text{ km}$) area-averaged surface flux (sensible + latent, W s^{-1}) during the 4-day period of 17/00–00 to 21/00–96 from the numerical experiments of CTL (thick solid), MV2 (long dashed), WV2 (thin solid), WSS1 (short-long dashed), WST_V2 (double-dot-dashed), RPVF (dotted), and RFRC (dot-dashed).

a. Effects of the vortex merger

After removal of V_1 (MV2), V_2 is organized mainly as a result of the mergers of many small-scale vortices within its own circulation (see Figs. 2 and 3 in Part II), as it is rolled up poleward as a tail of the ITCZ. The storm moves initially north-northeastward, following closely the CTL track, but turns sharply northwestward to the south of the CTL track after 18/15–39 (see Fig. 5b). Furthermore, in the absence of V_1 , the northwestward movement of the storm becomes much slower than in CTL. We attribute both the slower movement and the southward deflection of the MV2 storm to the simulated weaker intensity (Fig. 4). That is, the storm's weaker circulation (plus a smaller circulation size) tends to decrease its northward beta drift (Li and Wang 1994), thus reducing the influence of the upper-level flows in the sheared environment.

As expected, the development of V_2 alone does not show any evidence of sharp increases in surface winds, surface heat fluxes, or cyclonic vorticity during its life cycle (see Figs. 4 and 6). Instead, all the surface fields show relatively smooth variations with an initial slow deepening, followed by a period of slow dissipation. In the absence of V_1 , the MV2 storm is 9 hPa and 17 m s^{-1} weaker than the CTL one. This result confirms our conclusion reached in Part II that it is the vortex merger that is responsible for the sharp drop in central pressure and sharp increases in surface winds and heat fluxes after 18/15–39 in CTL. It is of interest to note, however, that despite the presence of an unfavorable environment, the MV2 storm could still continue its intensification, albeit at a slow rate, until 19/15–63, when the maximum surface wind reaches 20 m s^{-1} (Fig. 4b). This slow intensification

appears to be attributable to the continuous PV supply from the ITCZ. This result suggests that even though the ITCZ breakdown gives rise to a mesovortex as a precursor of TCG, its subsequent intensification would depend on many environmental conditions, such as vertical shear, SST, relative humidity, and, more importantly, the merger of vortices of different sizes and the PV supply from the ITCZ in the present case.

With the inclusion of a weaker V_2 in the initial conditions (WV2), one may expect the merger to take place as in CTL and its subsequent development to follow closely the CTL storm in track and the MV2 storm in intensity. However, none of those scenarios occurs. Specifically, a new mesovortex emerges after 12 h into the integration, which shares many similarities to V_2 in CTL except for its weaker intensity (Fig. 4). Such a weak vortex appears to affect the development and movement of V_1 in two ways: one is to make V_1 (1–2 hPa) weaker and the other is to slow its movement such that V_1 is more distant from V_2 than in CTL at 18/03–27 (Fig. 7). As a result, V_1 deflects gradually to the north away from V_2 and fails to merge with V_2 at the later time (see Figs. 7b and 5d). The development of such a weaker, slower-moving vortex, at first glance, cannot be directly related to the initially removed subvortex in V_2 . An examination of the CTL and WV2 simulations indicates that the weaker V_2 circulation tends to transport less high- θ_e (equivalent potential temperature) air from the ITCZ northeastward to feed deep convection developing within V_1 , thereby spinning V_1 up at a slower rate. (See Figs. 5c and 14 in Part I for the general distribution of θ_e in the vicinity of the ITCZ.) Thus, both vortices contain weaker cross-isobaric inflows in the PBL to attract each other even when they are about to be coalesced at their outskirts (Fig. 7b). Instead, the rotational flow of V_2 tends to advect V_1 northward through the vortex–vortex interaction, while the latter is under the influence of the larger-scale southeasterly flow. This leads to the northward drift of V_1 into the Mexican coast after 18/06–30 (Fig. 5d), and V_1 weakens shortly after its landfall. Since Table 1 and Fig. 4 show only the intensity of a mesovortex moving over the ocean, the WV2 storm associated with V_2 is 10 hPa and 18 m s^{-1} weaker than the CTL one because of the absence of the merging events; the former is even slightly weaker than the MV2 storm without the influence of V_1 .

A comparison of the MV2, WV2, and CTL storms could reveal different roles of V_1 and V_2 during the genesis of Eugene. That is, V_2 provides a favorable mesoscale circulation that feeds more high- θ_e air to convective activity within V_1 , whereas V_1 helps amplify the merger such that its low-level circulation could attain necessary strength to trigger the air–sea feedback

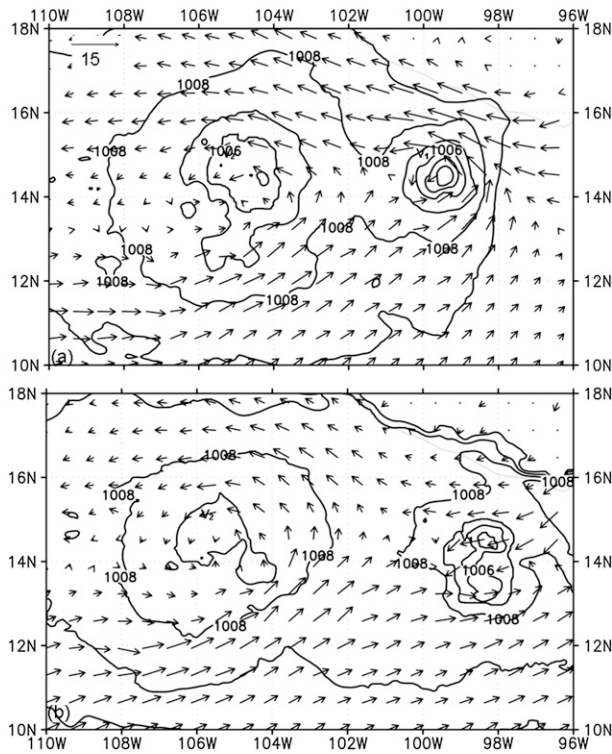


FIG. 7. Horizontal distribution of surface flow vectors [the reference vector is at the top left corner of (a), m s^{-1}], and the sea level pressure at intervals of 1 hPa, from the (a) CTL and (b) WV2 simulations at 18/03–27.

processes. Their mutual attraction leading to the final merger requires strong cross-isobaric inflows associated with both vortices. In this regard, one can see how delicate such a vortex–vortex interaction would be to the genesis (and predictability) of Eugene in the absence of a larger-scale cyclonic background as in RH97. The result also reveals that while the ITCZ breakdown and its subsequent rollup provide favorable conditions for the development of V_2 , it is unable to intensify to TS intensity without merging with V_1 unless it can be maintained over the warm tropical ocean surface. The time scale for V_2 to reach TS strength without merging with V_1 is about 3 days as seen from WST_V2, indicating again the critical roles of the vortex merger in the genesis of Eugene over a shorter time period.

b. Effects of warmer SST

When Eugene is allowed to move northwestward over “a tropical ocean surface” (WSST), it can still intensify even after 19/12–60 and reaches hurricane strength at 19/15–63 (Fig. 4). Its final intensity at 21/00–96 is 969 hPa (and 52 m s^{-1}), which is 17 hPa (and 14 m s^{-1}) deeper than the lowest surface central pressure during

the life cycle of the CTL storm (Table 1). This confirms the importance of warm SST in the TC development or, conversely, the role of colder SSTs in the dissipation of Eugene after its northwestward displacement away from the warm tropical ocean.

The role of SST can also be examined by comparing results between MV2 and WST_V2. One can see from Fig. 4 that although V_2 in WST_V2 intensifies slowly at first as in MV2, it begins to amplify more significantly after 20/06–78 as it keeps moving over a “tropical ocean” surface despite the presence of a strong sheared environment (see Fig. 7 in Part I), as do the storm-scale surface heat fluxes (not shown). Eventually, it reaches hurricane intensity with a maximum surface wind of 35 m s^{-1} . Note that the two pairs of the storms (i.e., WSST versus CTL and WST_V2 versus MV2) begin to depart in intensity after 19/12–60 and 20/00–72, respectively (Fig. 4). The different timings could be attributed to the different moments the storms move into the modified SST surface, that is, a later response to the SST change for a slower-moving storm (i.e., WST_V2 with respect to MV2). Numerous observational and modeling studies (e.g., Gray 1968; Krishnamurthi et al. 1994; Jones 1995; Frank and Ritchie 2001; Davis and Bosart 2003) have shown that strong vertical wind shear is generally inimical to the development of TCs even in the presence of favorable SST. The continued deepening of both WSST and WST_V2 storms in the strong sheared environment is consistent with some recent studies showing that strong TCs may be resilient to the environmental vertical wind shear (Wang and Holland 1996; Jones 2004; Rogers et al. 2003; Zhu et al. 2004; Zhang and Kieu 2006).

c. Effects of the frictional convergence

Because the PBL friction is gradually reduced, starting from 17/18–18 (RFRC), the two mesovortices are still able to develop and merge near 18/15–39, which is similar to CTL, as designed (Fig. 5e). As expected, both the surface flows and heat fluxes indeed become stronger than those in CTL after 18/12–36, as the PBL friction diminishes (Figs. 2b and 6). This is especially true during the intensifying period of 18/15–39 and 19/12–60 in which the maximum surface wind and the area-averaged surface heat flux are, respectively, about 8 m s^{-1} and 60 W s^{-1} greater than those in CTL. If WISHE is a dominant process here, one would expect greater deepening of the storm. However, reducing the PBL friction results in persistently higher minimum sea level pressures than those in the CTL, with a peak difference of 11 hPa (see Table 1), despite the generated stronger surface winds and heat fluxes. This indicates that increasing the heat and moisture fluxes alone could not account fully for the intensification of Eugene unless there are corresponding

increases in the low-level convergence. Without the PBL convergence, the increased heat and moisture content are mostly advected around rather than inward and then upward in convective rainbands; the latter is a prerequisite for TCG.

Note that the above scenario differs from that obtained from a series of sensitivity simulations on the effects of using different surface friction coefficients on the intensity of Hurricane Andrew (1992) by Yau et al. (2004), who showed that entirely removing the surface friction produces the highest surface winds and heat fluxes and the lowest surface pressures. As demonstrated by the previous studies of quasi-balanced dynamics (e.g., Krishnamurthi et al. 1994; Zhang and Kieu 2006), the mass and moisture convergence in the PBL or the transverse circulation can be decomposed into separate contributions of the friction and diabatic heating in deep convection. The two different scenarios just indicate that the PBL friction plays a more important role than diabatic heating in converging the mass and high- θ_e air from the ITCZ during the present TCG stage. The opposite is true during the hurricane stage in which the latent heating could account for more than 60% of the radial inflows in the PBL (see Zhang and Kieu 2006). In addition, Yau et al. (2004) modified only the surface friction, whereas in RSFC the frictional tendency in the vertical columns is reduced, implying more pronounced reduction of the frictional effects than in the former case. The RSFC experiment suggests that while the vortex-merging dynamics are critical to the air–sea feedback processes as discussed in Part II, the PBL frictional convergence provides an important mechanism by which the high- θ_e air could be transported into the inner-core region for increased convective activity, leading to the deepening of Eugene.

We have also conducted several other sensitivity simulations similar to RFRC but with the parameter μ applied to the first 18-h integration (i.e., with the PBL friction reduced by e^{-1} by 17/18–18). It is found that V_1 begins to deviate from its control track shortly after 17/18–18, in a manner similar to that in WV2 (Fig. 5d), and the two vortices fail to be merged (not shown); this likely is due to the lack of “mutual attraction” through their convergent cross-isobaric flows in the PBL. It is well known that vortices of the same sign tend to attract each other when they are in close proximity, eventually leading to their merger (e.g., Fujiwhara 1921; Lander and Holland 1993; Montgomery and Enagonio 1998; Prieto et al. 2003; Kuo et al. 2008). Apparently, it is the frictional convergence in the PBL that helps accelerate the mutual attraction leading to the final merger of the two mesovortices herein, which is also likely the case in the other mergers (e.g., RH97). This result indicates further the delicate sensitivity of the merger to intensity,

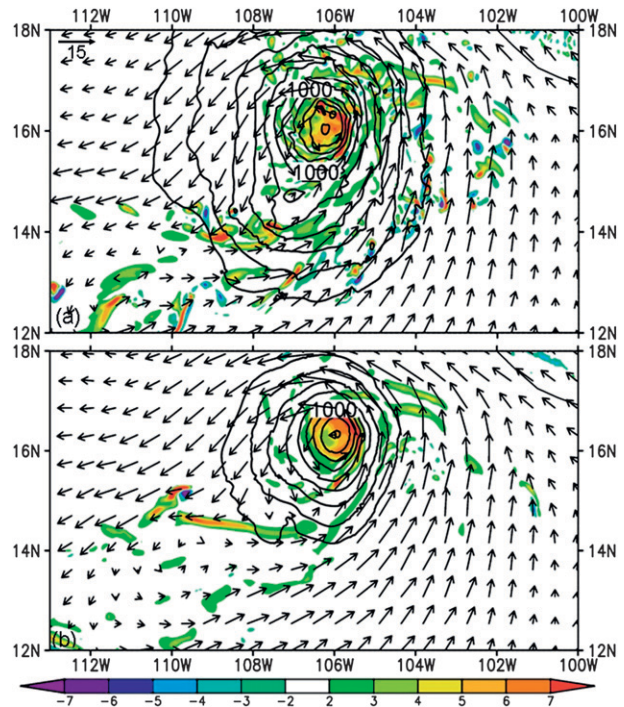


FIG. 8. Horizontal distribution of PV (shaded at intervals of 1 PVU) and flow vectors [the reference vector is at the top left corner of (a), m s^{-1}] at $z = 3$ km from the (a) CTL and (b) RPVF simulations at 19/00–48, superimposed with the sea level pressure field at intervals of 1 hPa.

size, and distance as well as to the physical processes occurring within the two mesovortices during the early stages of their life cycles.

d. Effects of the PV supplied from the ITCZ

As the PV fluxes at the southern boundary are reduced by a damping function after 18/15–39 (RPVF), the storm intensity is no longer comparable to the CTL storm. A snapshot of the horizontal distribution of PV at 19/00–48 from the CTL storm shows a “comma-shaped” structure with a “comma head” centered in the vortex circulation and a long “tail” of PV bands in the ITCZ (Fig. 8a). Clearly, most of the increased PV in the comma head comes from the PV bands in the ITCZ (see Figs. 2 and 6 in Part II). After activating the damping function, the PV bands in RPVF are substantially reduced in magnitude (cf. Figs. 8a,b), so the storm-integrated PV flux shows a sharp decrease immediately after the merger, followed by a sharp increase until 19/06–54 (Fig. 9). Although the PV flux still increases after the merger, it is on average about 60% less than that in CTL during the intensifying period. In this case, the increased PV flux is mostly from the convectively generated PV across the other three lateral boundaries, with

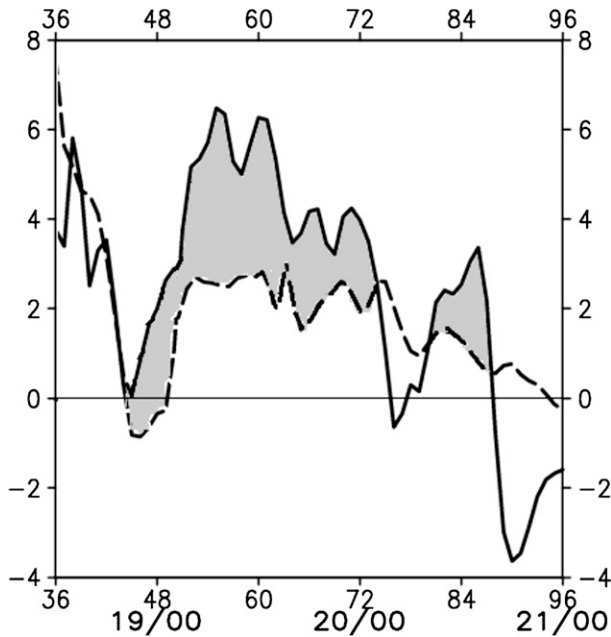


FIG. 9. Time series of the ($720 \text{ km} \times 720 \text{ km}$) area-averaged PV flux ($10^{-6} \text{ PVU s}^{-1}$), after being corrected by the domain movement, from the CTL (solid) and RPVF (dashed) simulations during the period of 18/12–36 to 21/00–96. Shaded areas denote the reduced portion of PV flux from the ITCZ in RPVF.

only a small portion from the southern boundary because of the way the damping function is defined.

It is evident from Fig. 4 that the second episode of intensification between 19/03–51 and 19/15–63, as shown in CTL, could no longer be observed after reducing the PV supply from the ITCZ. Table 1 shows that the minimum central pressure and the maximum surface wind, 9 hPa and 15 m s^{-1} , respectively, are weaker than those in CTL, as are the circulation intensity and size (cf. Figs. 8a,b). The effects of the PV bands in the ITCZ are similar to those associated with spiral rainbands of TCs as observed by May and Holland (1999). However, they could only speculate as to such an advective effect of PV on TC development because of their limited data. Our budget calculations presented in Part II and the sensitivity simulations shown herein confirm the early speculation of May and Holland and our conclusions given in Part II that the PV supply from the ITCZ plays an important role in maintaining the continued deepening of Eugene after it moves over the colder ocean surface. This suggests that the PV flux into the storm represents an essential process of the ITCZ rollup contributing to TCG. Without it, Eugene would indeed be much shorter lived in the presence of the strong vertical shear and colder SST, as hypothesized in Part II. At least, Eugene would likely begin to weaken soon after the merger.

4. Spinup of the cyclonic vorticity

One of the major conclusions obtained in Part II is that the spinup of cyclonic vorticity in Eugene occurs from the bottom upward during the merging period of 18/06–30 to 18/18–39 rather than from the top downward. While this seems to be obvious, given the fact that Eugene grows from a merger of a lower-level vortex (V_1) and a midlevel vortex (V_2), it still remains unclear how the surface cyclogenesis and the elevation of the peak vorticity depend on different processes (e.g., merging, friction). In this regard, several sensitivity simulations presented herein could provide different storm realizations and perspectives into the amplification of cyclonic vorticity leading to TCG. For this purpose, the results from MV2, WST_V2, and RFRC are compared to those in CTL, since the remaining three experiments are similar in many aspects to CTL except for their different intensities. In particular, in the first two experiments in which V_1 is removed, V_2 could intensify into TS strength, though at a slow rate, as a result of a merger of multiple small-scale vortices within a mesoscale circulation and the ITCZ rollup. The TCG scenarios in the two simulations (i.e., MV2 and WST_V2) appear to resemble to some extent those of RH97, except for their larger-sized mesovortices.

Figure 10 compares the height–time structures of the area-averaged absolute vorticity η (AAV) and lateral η -flux divergence, defined as $-\iint (\partial u \eta / \partial x + \partial v \eta / \partial y) dx dy$ [see Eq. (4) in Part II] from the abovementioned four experiments. The divergence of vertical-tilted horizontal vorticity is small, as shown in Fig. 9c in Part II, so the time rates of AAV changes are mainly caused by the lateral η -flux divergence. It is evident from Fig. 10a that the CTL storm begins with the AAV of about $3 \times 10^{-5} \text{ s}^{-1}$ below the melting level associated with V_2 , followed by a rapid vorticity growth during the merging phase and then a slow growth until reaching the maximum AAV of greater than $7.5 \times 10^{-5} \text{ s}^{-1}$ near 20/00–72. Of importance is that during the merging phase (i) the AAV isopleths are upright from the peak AAV level down to the surface and (ii) the vorticity growth due to the lateral η -flux divergence is peaked in the PBL. Subsequently, both the AAV and its flux divergence extend into a deep layer around the melting level, showing the bottom-up growth of AAV.

By comparison, the AAV in both the MV2 and WST_V2 simulations increases slowly with time, with the peak amplitudes located in the PBL; the two storms reach the peak AAV values at 19/18–66 and 20/15–87, respectively. Despite the different structures of AAV from those in CTL, it is interesting to note that the vorticity growth due to the lateral η -flux divergence is

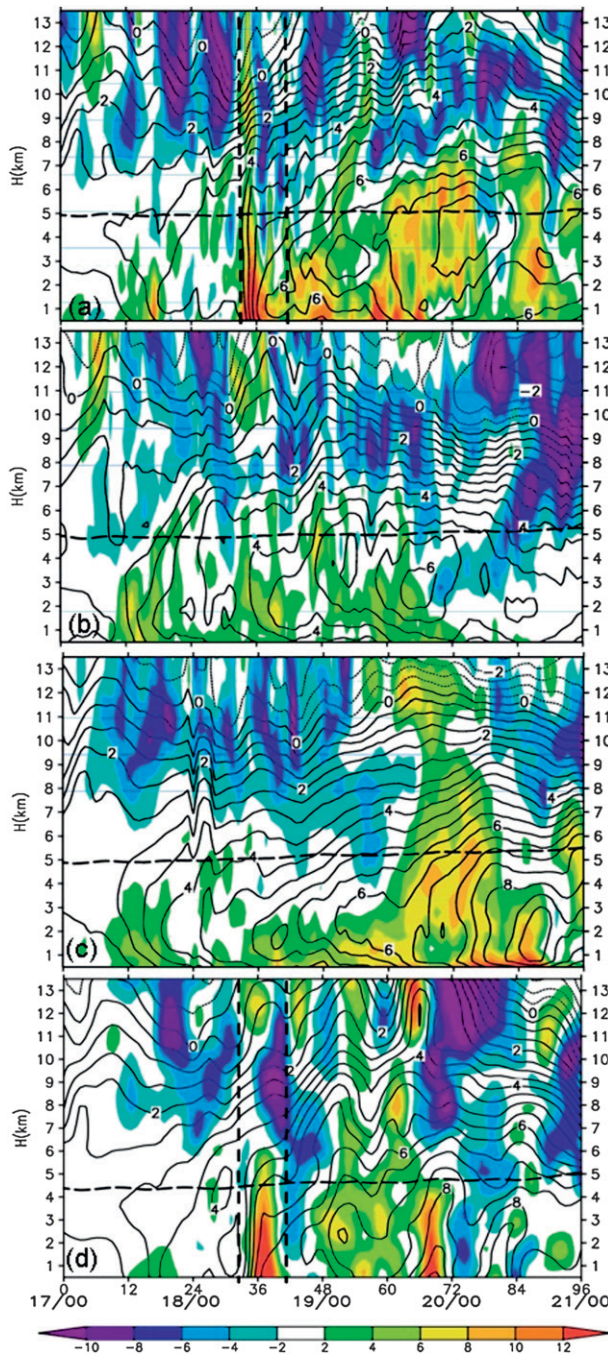


FIG. 10. Height–time cross sections of the ($720 \text{ km} \times 720 \text{ km}$) area-averaged absolute vorticity (contoured at intervals of $0.5 \times 10^{-5} \text{ s}^{-1}$) and the lateral η -flux divergence (shaded; every 10^{-10} s^{-2}) from the hourly model outputs of the (a) CTL, (b) MV2, (c) WST_V2, and (d) RFRC simulations. Horizontal thick dashed lines denote the melting level; vertical thick dashed lines denote the merging phase.

mostly peaked in the lowest 3-km layer (in MV2) or in the PBL (in WST_V2). There are two notable exceptions—one is the local η -flux divergence near the melting level around 19/00–48 in MV2 (Fig. 10b) and the other is the deep layer of η -flux divergence in WST_V2 during the period of 19/18–66 to 20/06–78 (Fig. 10c)—which are likely caused by the midlevel convergence associated with the latent heating above and melting cooling below, in contrast to the frictional convergence in the PBL. Note that such midlevel convergence differs from the AAV top-down hypothesis of RH97, which relies only on the dry dynamical processes through the increase of the penetration depth associated with the merger of midlevel PV. In all the cases, significant intensification of AAV occurs from the bottom upward during either the merging phase or the other development phases, although PV is always peaked at the melting level. Thus, we may state that even in the absence of a merger the AAV growth due to the η -flux divergence should be generally maximized in the PBL, with the AAV peaked between the PBL and melting level. Of course, the AAV cannot be maximized at the surface or in the PBL because of the frictional dissipation of the horizontal momentum.

The effects of the PBL friction on the spinup of AAV can be seen from the RFRC simulation (see Fig. 10d). First, gradually reducing the PBL friction, starting from 17/18–18, produces the peak AAV in the lowest layers, which is similar to the evolution of the tangential flows. Second, the vorticity growth due to the η -flux convergence occurs mostly below the melting level, also with the peak rates in the lowest layer. As discussed earlier, such low-level η -flux convergence must be closely related to radial inflows driven mostly by latent heating (e.g., Zhang and Kieu 2006). Because of this low-level lateral η -flux, the AAV grows at the fastest rate at the bottom where the central pressure (and gradient) is the deepest (strongest). Note that reducing the PBL frictional effects also decreases the moisture and mass convergence, which will in turn affect diabatic heating and consequently the vertical profiles of AAV. However, the bottom-up development of the cyclonic vorticity can be always expected once the convective heating becomes organized, as depicted by the quasi-balanced constraint of the Sawyer–Eliassen equation. This should also be the case even in the absence of surface friction, as shown in the other simulations (cf. Figs. 10a–d).

5. Summary and conclusions

In this study, several sensitivity simulations are performed to investigate the impact of various processes on the genesis of TS Eugene (2005) from the merging mesovortices associated with the ITCZ breakdowns and on

the subsequent vorticity growth and structures. They include the effects of removing one of the two mesovortices in each simulation, the impact of a warm SST surface, diminished friction in the PBL, and reduced PV supply from the ITCZ. The simulations confirm our conclusions obtained in Parts I and II that Eugene would not reach its observed TS intensity in the absence of the vortex merger and would become much shorter lived without the PV flux from the ITCZ.

Results reveal that although the ITCZ breakdowns (into mesovortices) and subsequent poleward rollup (through PV supply) provide favorable conditions for the initial genesis of Eugene, the mesoscale merger is more effective in the development of a self-sustaining tropical storm. Without the merger, it takes about 3 days for one of the mesovortices (i.e., V_2) to reach TS strength after imposing a tropical ocean surface along its track. The simulated Eugene can be transformed to hurricane intensity even in the presence of strong shear as long as it can be maintained over the same warm tropical ocean surface.

It is shown that when the model is initialized with a weaker V_2 due to the removal of a subvortex in it, V_1 becomes weaker and moves more slowly than in CTL. In particular, V_1 begins to deflect northward through the vortex–vortex interaction with V_2 when they are in close proximity, thereby failing to merge with V_2 . Without the merger, the model produces a storm that is 10 hPa higher and 18 m s^{-1} weaker than the CTL storm. The weaker intensity of V_1 appears to be attributable to the reduced transport of high- θ_e air for convective development as a result of the weaker circulation of V_2 , while the slower movement of V_1 is caused by the weaker cross-isobaric inflows in the PBL of both vortices such that the mutual attraction between them is weakened. The result reveals the subtle sensitivity of TCG from the vortex–vortex interaction and the vortex merger in the absence of a larger-scale organized flow.

When the PV flux from the ITCZ is reduced after the merger, the second episode of Eugene's intensification occurring after 19/03–51 could no longer be observed, leading to the development of a storm that is 9 hPa and 15 m s^{-1} weaker than the CTL one. The result indicates that the continuous PV supply into the “comma head” of Eugene's circulation represents the most favorable process of the ITCZ rollup contributing to TCG.

Results from our reduced friction experiment show the important role of the PBL friction in accelerating the mutual attraction of the two mesovortices leading to their final merger, given the steering flow associated with the ITCZ rollup interacting with a larger-scale southeasterly flow. With the reduced frictional convergence in the PBL at too earlier times, the two mesovortices tend to bifurcate in track and fail to eventually merge. When the

PBL friction is reduced after the merger, the simulated storm is 11 hPa higher than the CTL storm despite the generation of stronger surface winds and heat fluxes. This could be attributed to the decreased energy supply from the prestorm environment for convective development in the mesovortices.

It is found that the storm-scale cyclonic vorticity grows at the fastest rate in the PBL in all the simulations conducted in this study, including the CTL storm, because of the important contribution of the mass convergence from both the PBL friction and latent heating. The midlevel convergence associated with the latent heating above and melting below tends to provide a secondary maximum in the vorticity growth below the melting level. However, all results show consistently sharp increases in the vorticity growth during the merging phase, with the increasing absolute vorticity extending from the bottom upward with time. Thus, we may conclude that the growth of cyclonic vorticity during TCG tends to occur most likely from the bottom upward regardless of the mesovortex merger or a single mesovortex.

Acknowledgments. We thank three anonymous reviewers for their constructive and critical reviews, which helped improve the quality of this manuscript substantially. This work was supported by NASA Grant NNG05GR32G and NSF Grant ATM-0758609.

REFERENCES

- Charney, J. G., and A. Eliassen, 1964: On the growth of the hurricane depression. *J. Atmos. Sci.*, **21**, 68–75.
- Craig, G. C., and S. L. Gray, 1996: CISK or WISHE as the mechanism for tropical cyclone intensification. *J. Atmos. Sci.*, **53**, 3528–3540.
- Davis, C. A., and L. F. Bosart, 2003: Baroclinically induced tropical cyclogenesis. *Mon. Wea. Rev.*, **131**, 2730–2747.
- DeMaria, M., J. A. Knaff, and B. H. Connell, 2001: A tropical cyclone genesis parameter for the tropical Atlantic. *Wea. Forecasting*, **16**, 219–233.
- Elsberry, R. L., 1990: International experiments to study tropical cyclones in the western North Pacific. *Bull. Amer. Meteor. Soc.*, **71**, 1305–1315.
- Emanuel, K. A., 1987: An air–sea interaction model of intraseasonal oscillations in the tropics. *J. Atmos. Sci.*, **44**, 2324–2340.
- Frank, W. M., and E. A. Ritchie, 2001: Effects of vertical wind shear on the intensity and structure of numerically simulated hurricanes. *Mon. Wea. Rev.*, **129**, 2249–2269.
- Fujiwhara, S., 1921: The natural tendency towards symmetry of motion and its application as a principle in meteorology. *Quart. J. Roy. Meteor. Soc.*, **47**, 287–293.
- , 1923: On the growth and decay of vortical systems. *Quart. J. Roy. Meteor. Soc.*, **49**, 75–104.
- Gray, W. M., 1968: Global view of the origin of tropical disturbances and storms. *Mon. Wea. Rev.*, **96**, 669–700.
- Halverson, J., and Coauthors, 2007: NASA's Tropical Cloud Systems and Processes Experiment: Investigating tropical cyclogenesis

- and hurricane intensity change. *Bull. Amer. Meteor. Soc.*, **88**, 867–882.
- Hendricks, E. A., M. T. Montgomery, and C. A. Davis, 2004: The role of “vortical” hot towers in the formation of Tropical Cyclone Diana (1984). *J. Atmos. Sci.*, **61**, 1209–1232.
- Holland, G. J., and G. S. Dietachmayer, 1993: On the interaction of tropical-cyclone-scale vortices. III: Continuous barotropic vortices. *Quart. J. Roy. Meteor. Soc.*, **119**, 1381–1398.
- Hoskins, B. J., M. E. McIntyre, and A. W. Robertson, 1985: On the use and significance of isentropic potential vorticity maps. *Quart. J. Roy. Meteor. Soc.*, **111**, 877–946.
- Jones, S. C., 1995: The evolution of vortices in vertical shear. I: Initially barotropic vortices. *Quart. J. Roy. Meteor. Soc.*, **121**, 821–851.
- , 2004: On the ability of dry tropical-cyclone-like vortices to withstand vertical shear. *J. Atmos. Sci.*, **61**, 114–119.
- Kieu, C. Q., and D.-L. Zhang, 2008: Genesis of Tropical Storm Eugene (2005) associated with the ITCZ breakdowns. Part I: Observational and modeling analyses. *J. Atmos. Sci.*, **65**, 3419–3439.
- , and —, 2009: Genesis of Tropical Storm Eugene (2005) associated with the ITCZ breakdowns. Part II: Roles of vortex merger and ambient potential vorticity. *J. Atmos. Sci.*, **66**, 1980–1996.
- Krishnamurthi, T., H. Bedi, D. Oosterhof, and V. Hardiker, 1994: The formation of Hurricane Frederic of 1979. *Mon. Wea. Rev.*, **122**, 1050–1074.
- Kuo, H.-C., W. H. Schubert, C. L. Tsai, and Y.-F. Kuo, 2008: Vortex interactions and barotropic aspects of concentric eyewall formation. *Mon. Wea. Rev.*, **136**, 5183–5198.
- Kurihara, Y., M. A. Bender, and R. J. Ross, 1993: An initialization scheme of hurricane models by vortex specification. *Mon. Wea. Rev.*, **121**, 2030–2045.
- Lander, M., and G. J. Holland, 1993: On the interaction of tropical-cyclone-scale vortices. I: Observations. *Quart. J. Roy. Meteor. Soc.*, **119**, 1347–1361.
- Li, X., and B. Wang, 1994: Barotropic dynamics of the beta gyres and beta drift. *J. Atmos. Sci.*, **51**, 746–756.
- May, P. T., and G. J. Holland, 1999: The role of potential vorticity generation in tropical cyclone rainbands. *J. Atmos. Sci.*, **56**, 1224–1228.
- McBride, J. L., and R. Zehr, 1981: Observational analysis of tropical cyclone formation. Part II: Comparison of non-developing versus developing systems. *J. Atmos. Sci.*, **38**, 1132–1151.
- Molinari, J., D. Vollaro, S. Skubis, and M. Dickinson, 2000: Origins and mechanisms of eastern Pacific tropical cyclogenesis: A case study. *Mon. Wea. Rev.*, **128**, 125–139.
- Montgomery, M. T., and J. Enagonio, 1998: Tropical cyclogenesis via convectively forced vortex Rossby waves in a three-dimensional quasigeostrophic model. *J. Atmos. Sci.*, **55**, 3176–3207.
- Nieto Ferreira, R., and W. H. Schubert, 1997: Barotropic aspects of ITCZ breakdown. *J. Atmos. Sci.*, **54**, 261–285.
- Prieto, R., B. D. McNoldy, S. R. Fulton, and W. H. Schubert, 2003: A classification of binary tropical cyclone-like vortex interactions. *Mon. Wea. Rev.*, **131**, 2656–2666.
- Reasor, P. D., M. T. Montgomery, and L. F. Bosart, 2005: Mesoscale observations of the genesis of Hurricane Dolly (1996). *J. Atmos. Sci.*, **62**, 3151–3171.
- Ritchie, E. A., and G. J. Holland, 1993: On the interaction of tropical-cyclone-scale vortices. II. Discrete vortex patches. *Quart. J. Roy. Meteor. Soc.*, **119**, 1363–1379.
- , and —, 1997: Scale interactions during the formation of Typhoon Irving. *Mon. Wea. Rev.*, **125**, 1377–1396.
- Rogers, R. F., S. S. Chen, J. E. Tenerelli, and H. Willoughby, 2003: A numerical study of the impact of vertical shear on the distribution of rainfall in Hurricane Bonnie (1998). *Mon. Wea. Rev.*, **131**, 1577–1599.
- Serra, Y. L., and R. A. Houze Jr., 2002: Observations of variability on synoptic timescales in the east Pacific ITCZ. *J. Atmos. Sci.*, **59**, 1723–1743.
- Simpson, J., E. A. Ritchie, G. J. Holland, J. Halverson, and S. Stewart, 1997: Mesoscale interactions in tropical cyclone genesis. *Mon. Wea. Rev.*, **125**, 2643–2661.
- Stein, U., and P. Alpert, 1993: Factor separation in numerical simulations. *J. Atmos. Sci.*, **50**, 2107–2115.
- Wang, C. C., and G. Magnusdottir, 2006: The ITCZ in the central and eastern Pacific on synoptic time scales. *Mon. Wea. Rev.*, **134**, 1405–1421.
- Wang, Y., and G. J. Holland, 1995: On the interaction of tropical-cyclone-scale vortices. IV: Baroclinic vortices. *Quart. J. Roy. Meteor. Soc.*, **121**, 95–126.
- , and —, 1996: Tropical cyclone motion and evolution in vertical shear. *J. Atmos. Sci.*, **53**, 3313–3332.
- Yau, M. K., Y. Liu, D.-L. Zhang, and Y. Chen, 2004: A multiscale numerical study of Hurricane Andrew (1992). Part VI: Small-scale inner-core structures and wind streaks. *Mon. Wea. Rev.*, **132**, 1410–1433.
- Zhang, D.-L., and N. Bao, 1996a: Oceanic cyclogenesis as induced by a mesoscale convective system moving offshore. Part I: A 90-h real-data simulation. *Mon. Wea. Rev.*, **124**, 1449–1469.
- , and —, 1996b: Oceanic cyclogenesis as induced by a mesoscale convective system moving offshore. Part II: Genesis and thermodynamic transformation. *Mon. Wea. Rev.*, **124**, 2206–2226.
- , and C. Q. Kieu, 2006: Potential vorticity diagnosis of a simulated hurricane. Part II: Quasi-balanced contributions to forced secondary circulations. *J. Atmos. Sci.*, **63**, 2898–2914.
- Zhu, T., D.-L. Zhang, and F. Weng, 2004: Numerical simulation of Hurricane Bonnie (1998). Part I: Eyewall evolution and intensity changes. *Mon. Wea. Rev.*, **132**, 225–241.